Quantum Information and Computation, Vol. 11, No. 11&12 (2011) 0925–0936
© Rinton Press

LOW TEMPERATURE DYNAMICS OF NEUTRAL ATOMS FOR QUANTUM LOGIC

FANG-YU HONG
Department of Physics, Center for Optoelectronics Materials and Devices, Zhejiang Sci-Tech University
Xiasha College Park, Hangzhou, Zhejiang 310018, China

YANG XIANG
School of Physics and Electronics, Henan University
Kaifeng, Henan 475004, China

Z.Y. ZHU
Department of Physics, Center for Optoelectronics Materials and Devices, Zhejiang Sci-Tech University
Xiasha College Park, Hangzhou, Zhejiang 310018, China

W.H. TANG
Department of Physics, Center for Optoelectronics Materials and Devices, Zhejiang Sci-Tech University
Xiasha College Park, Hangzhou, Zhejiang 310018, China

Received November 20, 2010
Revised July 25, 2011

We study from the point of view of quantum logic the properties of the collective oscillations of two Rydberg atoms in two harmonic traps. The difference in the frequency of two normal modes of motion expands with the difference in the mass of the two atoms. The probability of excitation of the motional quanta due to the strong dipole-dipole interaction can be made to be sufficiently small. Based on the normal modes of motion we present a scheme for quantum state transfer which is useful for quantum information process and for precision spectroscopy of atoms that lack suitable transitions for efficient laser cooling, internal state preparation, and detection.

Keywords: normal mode, Rydberg state, quantum state transfer
Communicated by: S Braunstein & H Zbinden

1. INTRODUCTION

Quantum information science holds promise for many fascinating potential applications such as the factorization of large numbers[1], secure communication[2], and spectroscopic techniques with enhanced sensitivity [3]. Considering their extraordinary ability of quantum control and long coherence times, quantum optical systems like trapped ions [4, 5], neutral atoms [7, 6], and cavity QED [8, 9], have played prominent role in the implementing quantum information process in the laboratory. Proposals to build quantum computer with neutral atoms seem extremely promised because of very long coherence times of the internal atomic states and well-established techniques for cooling and trapping atoms in optical lattices [10], standard dipole traps [11], and magnetic microtraps [12]. Compared with trapped ions, neutral atoms have a huge advantage to turn on and off dipole interaction on demand with a

surprising contrast of 12 orders of magnitude, which makes the task of fabricating a scalable quantum register to be far easier than it may be for the trapped ions [13, 14].

To be a good qubit candidate, it should meet four key requirements: (i) possessing two levels being relatively immune to environmental perturbations;(ii) efficient cooling to minimize velocity-induced decoherence; (iii) faithful initial state preparation; (iv) accurate state detection. It is difficult to choose an atom that simultaneously fulfills these requirement. This difficulty can be overcome by choosing two different atomic species with one species only needing to have good immune levels and the other species fulfilling the other requirements [15]. For this two-species system normal modes of motions is a cornerstone of laser cooling and state transfer which is also essential to precision spectroscopy [15].

In this paper we discuss the dynamics of two neutral Rydberg atoms confined in two harmonic traps. The frequency difference between two normal modes increases with the difference in the mass of the two atoms. Based on normal modes of motion [16], we suggest a scheme for quantum state transfer from one atomic species to another. Though any unitary transformation U acting on n qubits can be composed from two-qubit CNOT gates and single-qubit rotation gates [17], there is a scheme for CNOT gates suggested by Jaksch *et al* based on Rydberg blockade between neutral atoms [18] and recently experimentally realized by Isenhower *et al* [19], and experimental $\sqrt{SWAP}$ entangling of neutral atoms mediated by collisions [20], it is not trivial to devise an efficient scheme for the state transfer between two neutral atoms.

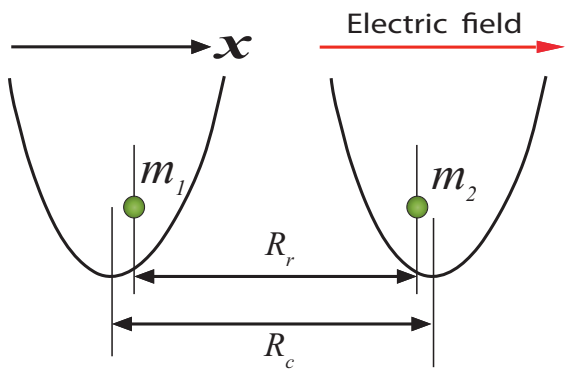

Fig. 1. (Color online) The degeneracy of the Rydberg states of two alkali atoms confined in two harmonic microtraps at distance R_c is removed by employing a constant electric field along the x direction.

2. DYNAMICS OF THE NORMAL MODE OF MOTION

Consider two atom 1 and 2 of mass m_1 and $m_2 = \gamma\, m_1\, (\gamma \geq 1)$, respectively, confined in two harmonic microtraps (see Fig.1). The atoms are excited to the Rydberg states of a principal quantum number n. To remove the degeneracy of the Rydberg state, a constant electric field

along the x axis is applied. The Rydberg state has a dipole moment [18]

$$\mu = \mu_z \mathbf{e}_x = \frac{3}{2} nqea_0 \mathbf{e}_x, \tag{1}$$

where q is a parabolic quantum number

$$q = n-1-|m|, n-3-|m|, \cdots, -(n-1-|m|) \tag{2}$$

with magnetic quantum number m. The two Rydberg atoms interact via the dipole-dipole potential

$$V_{dip}(\mathbf{r}) = \frac{\mathbf{1}}{\mathbf{4}\pi\epsilon_{\mathbf{0}}} \left[\frac{\mu_{\mathbf{1}} \cdot \mu_{\mathbf{2}}}{|\mathbf{r}|^{\mathbf{3}}} - \mathbf{3} \frac{(\mu_{\mathbf{1}} \cdot \mathbf{r})(\mu_{\mathbf{2}} \cdot \mathbf{r})}{|\mathbf{r}|^{\mathbf{5}}} \right], \tag{3}$$

where $\mathbf{r}$ is the distance between the two atoms. In this paper, we will assume that due to the sufficiently large electric field, the energy difference between two neighboring stark states is far larger than the dipole-dipole interaction and that the transitions $(m, m) \to (m \pm 1, m \mp 1)$ due to the nondiagonal terms of V_{dip} are suppressed by an appropriate choice of the initial stark eigenstate [18]. If two atoms are in the hydrogen Rydberg state

$$|r\rangle = |n, q = n-1, m = 0\rangle \tag{4}$$

one may find that

$$V_{dip}(R) = -9[n(n-1)]^2 (\frac{a_0}{R})^3 \frac{e^2}{8\pi\epsilon_0 a_0} \tag{5}$$

for a distance $\mathbf{r} = \mathbf{R}\mathbf{e_z}$. For alkali atoms n should be interpreted as an effective principle quantum number [21].

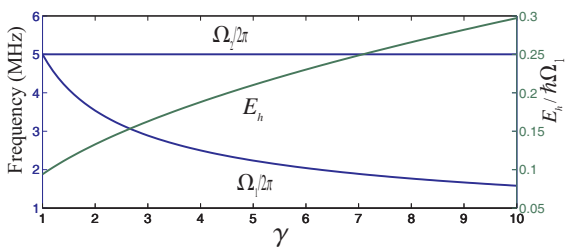

Fig. 2. (Color online) The frequencies $\Omega_{1,2}$ of the normal mode of the motion and the heat energy E_h versus the ratio $\gamma = m_2/m_1$. The relevant parameters are $n = 100$, $R_c = 8\,\mu$m, $\omega_{t1} = 2\pi \times 5$MHz, and $m_1 = 85.5$u.

We encode Qubits in two internal atomic ground states (e.g., hyperfine levels) $|g\rangle$ and $|s\rangle$. The distance between the centers $x_{ci}(i = 1, 2)$ of the two harmonic microtraps is $R_c = |\mathbf{x_{c1}} - \mathbf{x_{c2}}|$ (see Fig.1). $R_r = |\mathbf{x_{r1}} - \mathbf{x_{r2}}|$ denotes the distance between the equilibrium positions of the two atoms $x_{ri}(i = 1, 2)$ when they are in the Rydberg state $|r\rangle$. In the following we assume the harmonic potential of frequencies in the y and z directions is sufficiently strong that the motion along these directions can be neglected and we only need to consider the motion along the x direction. The atoms have been previously laser cooled in all three dimensions so

that they fluctuate around the equilibrium position. When the two atoms is excited to the Rydberg state $|r\rangle$, the potential energy of the system is given by

$$V(x_2 - x_1) = \sum_{i=1}^{2} \frac{1}{2} k_0 [x_i(t) - x_{ci}]^2 + \frac{A}{[x_2(t) - x_1(t)]^3}, \tag{6}$$

where x_i is the coordinate of the atom i and $k_0 = \omega_{t1}^2 \cdot m_1 = \omega_{t2}^2 \cdot m_2$ is a constant with $\omega_{ti}(i = 1, 2)$ being the frequencies of the ith microtrap , respectively, and the constant

$$A = -\frac{9[n(n-1)]^2 a_0^2 e^2}{8\pi\epsilon_0}. \tag{7}$$

The equilibrium positions of the two Rydberg atoms $x_{ri}(i = 1, 2)$ are the solutions of the equations $\partial V/\partial x_i = 0\,(i = 1, 2)$, i.e.

$$k_0(x_1 - x_{c1}) + \frac{3A}{(x_2 - x_1)^4} = 0, \tag{8}$$

and

$$k_0(x_2 - x_{c2}) - \frac{3A}{(x_2 - x_1)^4} = 0. \tag{9}$$

Those equations can be solved numerically if x_{ci} is given.

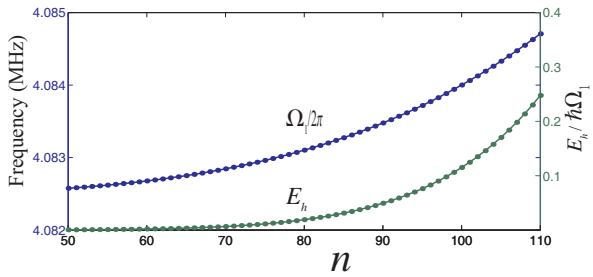

Fig. 3. (Color online) The frequencies Ω_1 of the normal mode of the motion and the heat energy E_h versus the principle quantum number n. The relevant parameters are $\gamma = 1.5$, $R_c = 8\,\mu$m, $\omega_{t1} = 2\pi \times 5$MHz, and $m_1 = 85.5$u.

Assuming the collective motions of the two atoms around the equilibrium position are small, we approximate V with its Taylor expansion around x_{ri} truncated to second order. The dynamics of the system are characterized by the Lagrangian

$$L = \frac{1}{2} \sum_{i=1}^{2} m_i \dot{q}_i^2 - \frac{1}{2} \sum_{i,j=1}^{2} V_{ij} q_i q_j, \tag{10}$$

where $q_i = x_i - x_{ri}$ are the displacements of the atoms from the equilibrium positions x_{ri}, and

$$\begin{aligned} V_{ij} = \frac{\partial^2}{\partial x_i \partial x_j} V(x_2 - x_1)|_{x_{ri}} &= k_0 + k_d \quad if \;\; i = j \\ &= -k_d \quad if \;\; i \neq j \end{aligned} \tag{11}$$

with

$$k_d = \frac{12A}{R_r^5}. \tag{12}$$

From Eq. (10), we have the equations for the normal modes of the motion

$$\sum_{j=1}^{2} V_{ij} b_\alpha^j = \lambda_\alpha m_i b_\alpha^i \quad with \; \alpha = 1, 2, \tag{13}$$

where the eigenvalues $\lambda_\alpha \geq 0$ since the matrix V_{ij} is real, symmetric, and non-negative definite, and b_α is the eigenvector at λ_α. The frequency of the normal mode α is $\Omega_\alpha = \sqrt{\lambda_\alpha}$. Introducing the mass-weighted coordinates $q_i' = \sqrt{m_i} q_i$, we can rewritten the eigenvalue problem as

$$\sum_{j=1}^{2} V_{ij}' \, b_\alpha^{j\prime} = \Omega_\alpha^2 \, b_\alpha^{i\prime} \quad for \; \alpha = 1, 2, \tag{14}$$

where $V_{ij}' = V_{ij}/\sqrt{m_i m_j}$ [22, 23].

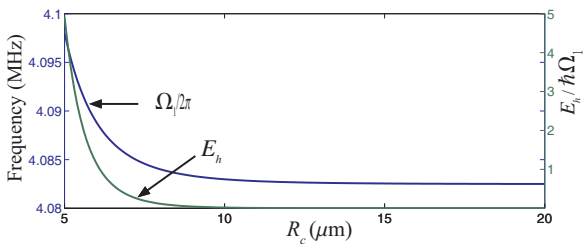

Fig. 4. (Color online) The frequencies Ω_1 of the normal mode of the motion and the heat energy E_h versus the distance between the centers of the two microtraps R_c. The relevant parameters are $n = 100$, $\gamma = 1.5$, $\omega_{t1} = 2\pi \times 5$MHz, and $m_1 = 85.5$u.

Solving the secular equation (14) gives the eigenfrequencies of the motion

$$\Omega_1 = \frac{1}{2m_1} \left[(k_0 + k_d)(1 + \frac{1}{\gamma}) - \sqrt{(k_0 + k_d)^2 (1 - \frac{1}{\gamma})^2 + 4 \frac{k_d^2}{\gamma}} \right] \tag{15}$$

and

$$\Omega_2 = \frac{1}{2m_1} \left[(k_0 + k_d)(1 + \frac{1}{\gamma}) + \sqrt{(k_0 + k_d)^2 (1 - \frac{1}{\gamma})^2 + 4 \frac{k_d^2}{\gamma}} \right] \tag{16}$$

with corresponding displacements

$$b_1 = N_1 \left(\sqrt{\gamma}, -\frac{1}{4} \left[3(1-\gamma) - \sqrt{9(1-\gamma)^2 + 16\gamma} \right] \right) \tag{17}$$

and

$$b_2 = N_2 \left(\sqrt{\gamma}, -\frac{1}{4} \left[3(1-\gamma) + \sqrt{9(1-\gamma)^2 + 16\gamma} \right] \right), \tag{18}$$

where the first and second components describe the motion of atom 1 and 2, respectively. Here, the constant $N_{1,2}$ are the normalization factor, satisfying the scalar products

$$b_1^i b_1^j + \gamma b_2^i b_2^j = \delta_{ij} \quad with\ i,j = 1,2, \tag{19}$$

and

$$b_i^1 b_j^1 + \gamma b_i^2 b_j^2 = \delta_{ij} \quad with\ i,j = 1,2. \tag{20}$$

In Fig. (2, 3, 4) we plot the eigenfrequencies as a function of γ, the principle quantum number n, and the distance between the two center of the harmonic microtraps.

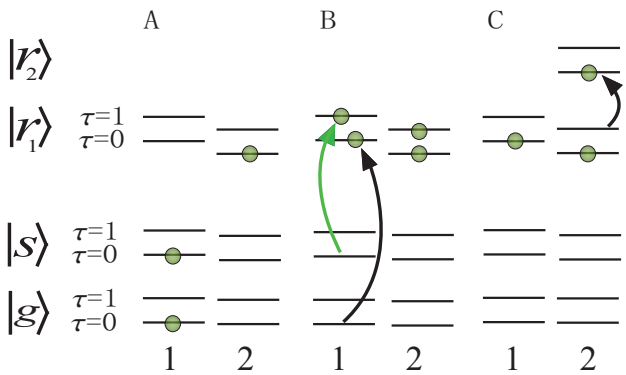

Fig. 5. (Color online) Quantum state transfer scheme for two atoms sharing a common normal mode of motion with τ denoting the number of the excitation of the normal mode Ω_1. See text for explanation.

The normal modes of the atom motion are defined by

$$Q_i(t) = \sum_{j=1}^{2} b_i^j q_j'(t). \tag{21}$$

In terms of the normal modes of the motion the Lagrangian for the atoms oscillations Eq.(10) may be rewritten as

$$L = \frac{1}{2} \left[\sum_{i=1}^{2} \left(\dot{Q}_i^2 - \Omega_i^2 Q_i^2 \right) \right]. \tag{22}$$

From this expression we see that the modes Q_i are uncoupled, thus we have the Hamiltonian

$$H = \frac{1}{2} \left[\sum_{i=1}^{2} \left(P_i^2 + \Omega_i^2 Q_i^2 \right) \right] \tag{23}$$

with the canonical momentum $P_i = \dot{Q}_i$. By introducing the operators

$$Q_j \to \hat{Q}_j = \sqrt{\frac{\hbar}{2\Omega_j}}(a_j + \hat{a}_j^\dagger) \quad with\ j = 1, 2, \tag{24}$$

and

$$P_j \to \hat{P}_j = i\sqrt{\frac{\hbar}{2\Omega_j}}(a_j - \hat{a}_j^\dagger) \quad with\ j = 1, 2, \tag{25}$$

where the annihilation and creation operators $\hat{a}_j$ and $\hat{a}_j^\dagger$ obey the usual commutation relation $[\hat{a}_i, \hat{a}_j^\dagger] = \delta_{ij}$ and $\hat{Q}_j$ and $\hat{P}_j$ satisfy the canonical commutation relation $[\hat{Q}_i, \hat{P}_j] = i\hbar\delta_{ij}$. From Eqs. (21, 24), we have

$$q_i = \frac{1}{\sqrt{m_i}} \sum_{\alpha=1}^{2} (b_\alpha^i)^{-1} \sqrt{\frac{\hbar}{2\Omega_\alpha}}(a_\alpha + a_\alpha^\dagger). \tag{26}$$

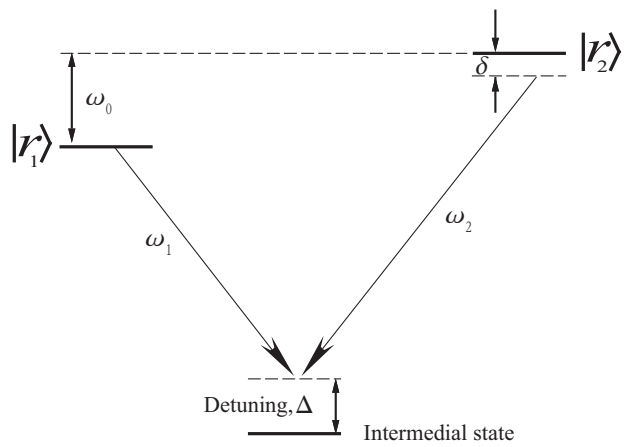

Fig. 6. (Color online) The relevant levels and laser pulses for the stimulated Raman transition $|r_1, 1\rangle \to |r_2, 0\rangle$ [24].

When both atoms are excited to the Rydberg state the mechanical force due to V_{dip}

$$F_{dip} = \frac{dV_{dip}(R)}{dR}|_{R=R_0} = -\frac{3A}{R_0^4} \tag{27}$$

will heat the two-atom system. Considering the contribution from the harmonic microtraps the heat energy can be estimated by

$$E_h = -\frac{1}{4}k_0(R_r - R_c)^2 + \frac{3A}{R_r^4}(R_r - R_c) \tag{28}$$

for a duration of $\pi/2\Omega_1$ [25]. In Fig. (2, 3, 4) we also plot E_h in unit of the spacing of the normal mode $\Delta E_{nm} = \hbar\Omega_1$ as a function of the mass ratio γ, the principle quantum number n, and the distance between the two center of the harmonic traps.

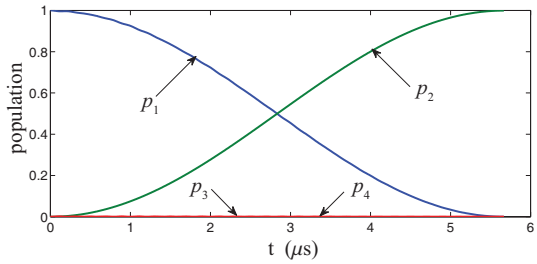

Fig. 7. (Color online) The simulation of the atomic state evolution $|r_1, 1\rangle \to |r_2, 0\rangle$ under a π laser pulse illumination, assuming $\delta = \Omega_1 = 2\pi \times 4$ MHz, $\Omega_2 = 2\pi \times 5$ MHz, $\Delta = 2\pi \times 100$GHz, $g_1 = g_2 = 2\pi \times 10^2$MHz, $t_d = 5.67\mu$s, $\phi_1 = \phi_2$, $\eta = 0.5$, $\Gamma = 2$ KHz.

Fig.2 shows that with the increasing of γ, the normal mode frequency Ω_1 decreases and Ω_2 changes little, and the heat E_h increases with γ but remained small for the given parameters. Ω_1 and E_h increase with the principle quantum number n (Fig. 3). We have $E_h > \hbar\Omega_1$ if $R_c < 6.1\mu$m (Fig. 4). Assuming $m_1 = 85.5$ u (the atomic mass unit), $n = 100$, $\gamma = 1.5$, $R_c = 8\mu$m, $\omega_{t1} = 2\pi \times 5$ MHz, and $\omega_{t2} = \omega_{t1}/\sqrt{\gamma} = 2\pi \times 4.082$ MHz, we have $R_r = 7.997\mu$m, $\Omega_1/2\pi = 4.084$MHz, $\Omega_2/2\pi = 5.002$MHz. Though the frequencies of the normal modes $\Omega_{1,2}$ are only slightly different from the two trap frequencies $\omega_{ti}(i = 1, 2)$, the dipole-dipole interaction has an important role in the motion of normal modes, since the work done by this interaction is

$$W_d = -\frac{3A}{(x_{r2} - x_{r1})^4}(x_{r1} - x_{c1}) - \frac{3A}{(x_{r2} - x_{r1})^4}(x_{c2} - x_{r2}), \tag{29}$$

the work done by the traps on the two atoms from $x_{ci}(i = 1, 2)$ to $x_{ri}(i = 1, 2)$ approximately equals

$$W_t = \sum_{i=1}^{2} \frac{1}{2} k_0 (x_{ri} - x_{ci})^2, \tag{30}$$

and we have $W_d = 2W_t$ according to Eqs (8,9). The normal modes are collective modes shared by the two atoms and can be used for quantum information transfer between two qubits. The fluctuation of the coordinate of m_1 is $\Delta x_1 = \sqrt{\hbar/2m_1\Omega_1} = 3.4$ nm which is very small and its effect on the normal motion can be safely neglected, and the heating energy $E_h/\hbar\Omega_1 = 0.12$ is small and can be neglected considering that it will average to zero over a whole period $2\pi/\Omega_1$.

3. SCHEMES FOR QUANTUM LOGIC

Now we discuss a possible application of the normal modes of motion of two neutral atoms based on the strong dipole-dipole interaction. Quantum state transfer between two qubits is essential to a quantum computer, a quantum network, and precision spectroscopy of atoms that lack suitable transitions for efficient laser cooling [22, 26], internal state preparation, and detection. We assume that the two atom 1 and 2 are initially in the state

$$|\psi\rangle_1 = (\alpha|g\rangle_1 + \beta|s\rangle_1)|r_1\rangle_2 \tag{31}$$

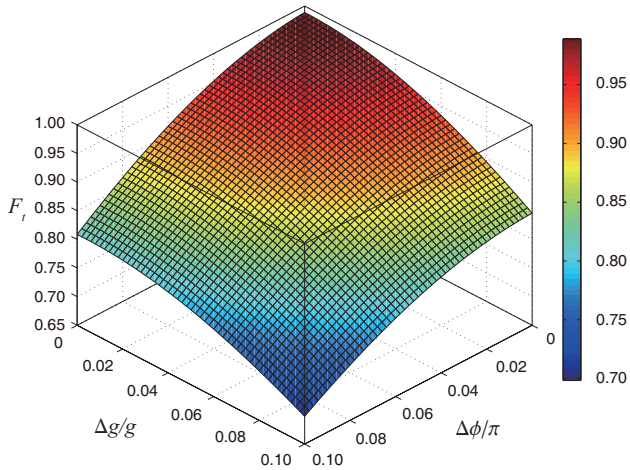

Fig. 8. (Color online) The effects of errors in the coupling $g_i (i = 1, 2)$ and phase difference ϕ on the fidelity of transferring state $|\phi\rangle_1 = (|s\rangle_1 + |g\rangle_1)/\sqrt{2}$ of atom 1 to atom 2 with $\Delta g_1 = \Delta g_2 = \Delta g$ and other parameters remained the same as those in figure 7. The maximum of state transfer fidelity $F_{tmax} = 0.988$.

where $|\alpha|^2 + |\beta|^2 = 1$, and that all the motional mode are initially cooled to near their ground state by Raman sideband cooling on atoms [27](Fig. 5A). We now drive a π pulse on transition $|g\rangle|0\rangle \leftrightarrow |r_1\rangle|0\rangle$ on atom m_1 leading to

$$|\psi\rangle_1 \rightarrow |\psi\rangle_2 = \alpha|r_1\rangle_1|r_1\rangle_2|0\rangle + \beta|s\rangle_1|r_1\rangle_2|0\rangle. \tag{32}$$

where we have used the fact that the normal mode of motion is shared by atoms m_1 and m_2 and assumed the motional mode are still in their ground state considering that $E_h/\hbar\Omega_1$ is small. Then a blue sideband (BSB) π pulse on transition $|s\rangle|0\rangle \leftrightarrow |r_1\rangle|1\rangle$ is applied to atom m_1 leading to

$$|\psi\rangle_2 \rightarrow |\psi\rangle_3 = \alpha|r_1\rangle_1|r_1\rangle_2|0\rangle + \beta|r_1\rangle_1|r_1\rangle_2|1\rangle \tag{33}$$

(Fig. 5B). During the BSB pulse duration, the $|r_1\rangle_1|0\rangle$ component of the wave function is not affected since the state $|s\rangle_1|-1\rangle$ is nonexistent [28, 29], which is the vital element of quantum logic employed in literatures [15, 27, 30].

Then a π pulse tuned to the transition $|r_1\rangle_2|1\rangle \rightarrow |r_2\rangle|0\rangle$ is applied to atom 2 leading to

$$|\psi\rangle_2 \rightarrow |\psi\rangle_3 = |r_1\rangle_1(\alpha|r_1\rangle_2 + \beta|r_2\rangle_2)|0\rangle. \tag{34}$$

Thus the quantum state of atom 1 has been transferred to atom 2 (Fig. 5C). The Rydberg state $\alpha|r_1\rangle_2 + \beta|r_2\rangle_2$ is then transferred to the ground state $\alpha|g\rangle_2 + \beta\,|s\rangle_2$, which concludes the state transfer. The last state can be efficiently measured by projecting its state to $|g\rangle$ and $|s\rangle$.

Based on the state transfer operations, we can measure single-laser pulse (Rabi) spectroscopy of atom 1. First we make a frequency scan across the resonance by applying to atom 1 interrogation pulses of constant intensity and duration, corresponding to π pulses on the

transition $|g\rangle \leftrightarrow |s\rangle$ when the laser beam was tuned to resonance. So the coefficient α and β is dependent on the frequency of the interrogation pulses. Then we perform the aforesaid state transfer operations and read out the states of atom 2. By repeating this experiments many times for a given interrogation pulse frequency, the probabilities $|\alpha|^2$ and $|\beta|^2$ as functions of the spectroscopy probe frequency can be determined and therefrom the transition frequency of atom 1 is measured [15]. For example, many wavelengths like 6822.4 $\mathring{A}$ of transition $|s\rangle_1 = 4p^5 5s5p$ 4S $\leftrightarrow |g\rangle_1 = 4p^5 4d(^3\mathrm{D})5s$ 2D° in ^{87}Rb are not accurate [31], we can take ^{87}Rb and ^{133}Cs as atom 1 and 2, respectively, then transfer state $|\phi\rangle_1 = \alpha|g\rangle_1 + \beta|s\rangle_1$ to atom 2, $|\phi\rangle_2 = \alpha|g\rangle_2 + \beta|s\rangle_2$ with $|g\rangle_2 = |F, m_F\rangle = |3, 0\rangle$ and $|s\rangle_2 = |4, 0\rangle$ to accurately measure the transition frequency with the aid of ^{133}Cs [32].

Table 1. Effect of errors in parameters on the fidelity of the state transfer of $|\phi\rangle_1$. The parameters remain the same as those used in figure 7. When there are no errors, the fidelity of the state transfer is $F = 0.995$ for the transform $|r_1, 1\rangle \to |r_2, 0\rangle$ and $F = 0.999$ for $|g, 0\rangle \to |r_1, 0\rangle$, respectively.

Err	10% g_1	10% g_2	10% Δ	10% η	$\Delta\delta^a$	$\Delta\phi$	10% t_d	200%$\Delta\Gamma$
F	0.881	0.909	0.987	0.992	0.965	0.981	0.989	0.990
Err	10% g_1	10% g_2	10% Δ	10% η	$\Delta\delta^b$	$\Delta\phi$	10% t_d	200%$\Delta\Gamma$
F	0.968	0.971	0.991	0.998	0.993	0.975	0.993	0.997

Now we numerically simulate the state transfer of an unknown state from a qubit to another. We assume state rotations are performed on $|a, j\rangle \leftrightarrow |b, k\rangle (a, b = s, g, r_1, r_2, j, k = 0, 1)$ transition with two-photon stimulated Raman (TWSR) pulses described by $\mathbf{E}_i \propto g_i[exp\,(i\mathbf{k}_i \cdot \mathbf{x} - i\omega_i t + i\,\phi_i) + cc](i = 1, 2)$ [27, 33] . The relevant levels for the stimulated Raman transition $|r_1, 1\rangle \to |r_2, 0\rangle$ is shown in the Fig.6 [24]. After we adiabatically eliminate the intermediate state through the standard method, the effective Hamiltonian describing the transition $|r_1, 1\rangle \leftrightarrow |r_2, 0\rangle$ has the following form in the interaction picture[24]

$$\begin{aligned} H_I &= -i\eta\hbar\frac{\Omega_0}{2}a_1\sigma_+ exp\,(i\phi) - \hbar\frac{\Omega_0}{2}\sigma_+ exp\,(i\phi + i\Omega_1 t) \\ &- \hbar\frac{\Omega_0}{2}\sigma_+ exp\,(i\phi + i\Omega_2 t) + h.c., \end{aligned} \tag{35}$$

where $\Omega_0 = 2|g_1 g_2|/\Delta$ with the detuning Δ shown in Fig.6, $\phi = \phi_1 - \phi_2$, and $\sigma_+ = |r_2\rangle\langle r_1|$. Here we have considered the effect arising from the levels $|r_2, 1\rangle$ and $|r_2, 1_2\rangle$ with $|1_2\rangle$ being an excitation in the normal mode Ω_2. In Fig.7, assuming the pertinent Rydberg states spontaneously decay with a rate $\Gamma = 2$ KHz [13] we simulate a π state rotation $|r_1, 1\rangle \to |r_2, 0\rangle$ with realistic parameters $\delta = \Omega_1 = 2\pi \times 4$ MHz, $\Omega_2 = 2\pi \times 5$ MHz, $\Delta = 2\pi \times 100$GHz, Rabi frequencies of two pulses $g_1 = g_2 = 2\pi \times 10^2$MHz, pulse duration $t_d = 5.67\mu$s, initial phase $\phi_1 = \phi_2$, the Lamb-Dicke parameter $\eta = 0.5$ [19, 34]. Here p_2 denotes the population in the level $|r_2, 0\rangle$, p_3 and p_4, respectively, denote the population in the level $|r_2, 1\rangle$ and $|r_2, 1_2\rangle$. Therefrom we see that the possibility ($< 1.4\%$) of excitations to levels other than $|r_2, 0\rangle$ is negligible.

The effect of unknown experimental errors from the two-photon stimulated Raman pulses on the fidelity of the state transfer is shown in the table **??**, where the first line describes

the errors from the transformation $|r_1, 1\rangle \to |r_2, 0\rangle$, the third line describes the errors from the transformation $|g, 0\rangle \to |r_1, 0\rangle$, with $\Delta\delta^a = \pm 2\pi \times 10$KHz, $\Delta\delta^b = \pm 2\pi \times 2$KHz, and $\Delta\phi = \phi_1 - \phi_2 = \pm 0.1\pi$. The effect of Errors from the other pulses during the state transfer on the fidelity F are similar to those shown in the table **??**. The fidelity F decrease by less than 0.5% when the decay rate increase by two times. In figure 8 we numerically estimate the effects of the errors in the coupling $g_i (i = 1, 2)$ and phase difference ϕ on the transfer fidelity F_t of state $|\phi\rangle_1 = (|s\rangle_1 + |g\rangle_1)/\sqrt{2}$ to atom 2. The system of two neutral atoms is robust against unknown experimental errors in the parameters.

The probability of spontaneous emission during a π TWSR pulse $p_{se} \simeq \pi/(2\Delta\tau_l)$ with τ_l the intermediate state lifetime [25]. Assuming $\tau_l = 10$ ns gives $p_{se} \simeq 5 \times 10^{-4}$. Other experimental imperfections including background gas collisions, photon scattering, laser noise induced heating, AC Stark shifts, and background fields may influence the coherence of the qubit states and limit the coherence time to be on the order of a second [25]. Thus the effect on the state transfer due to these experimental imperfections are negligible. To trap both ground and Rydberg state atoms one can use the blue-detuned far-off-resonance optical traps (FORTs), which will also help to improve the Rydberg state lifetime [25].

4. CONCLUSION

We have discussed the normal mode of motion of two neutral Rydberg atoms based on the strong dipole-dipole interaction. The frequencies of the two normal modes of motion are slightly larger than that of the two traps. To suppress the excitation of the motional quanta the heat energy arising from the strong dipole-dipole interaction can be controlled to be sufficiently small. Possible application of the normal modes of motion can be found in the laser cooling, state transfer, and precise spectroscopy. In quantum information process and precise spectroscopy, it is rather difficult to find a candidate neutral atom which has long-lived and reliably initialized levels, at the same time can be efficiently cooled and detected precisely. With this normal-mode-based state transfer scheme, one atom needs only have a good level structure and the other atom satisfies the other requirements.

Acknowledgements

This work was supported by the National Nature Science Foundation of China (Grant No.10874071, 11072218, 11005031, 50672088, and 60571029), by Zhejiang Provincial Natural Science Foundation of China (Grant No. Y6110314), by Scientific Research Fund of Zhejiang Provincial Education Department (Grant No.Y200909693), and by Science Foundation of Zhejiang Sci-Tech University (ZSTU) under Grant No.0913842-Y.

References

1. P.W. Shor, in *Proceeding of the 35th Annual Symposium on the Foundations of Computer Science*, edited by S. Goldwasser (IEEE Computer Society, Los Alamitos, CA), 124 (1994). Expanded version of this paper is available at arXiv: quant-ph/9508027.
2. A. Ekert, Phys. Rev. Lett. **67**, 661 (1991).
3. D. Ulam-Orgikh and M. Kitagawa, Phys. Rev. A **64**, 052106 (2001).
4. C. Sackett *et al.*, Nature (London) **404**, 256 (2000).
5. R. Blatt and D. Wineland, Nature (London) **453**, 1008 (2008).

6. I. Bloch, Nature (London) **453**, 1016 (2008).
7. H.-J Briegel *et al.*, J. Mod. Opt. **47**, 415 (2000).
8. C. Hood *et al.*, Science **287**, 1447 (2000); A. Rauschenbeutel *et al.*, Phys. Rev. Lett. **83**, 5166 (2000)
9. C. Barthel, D.J. Reilly, C.M. Marcus, M.P. Hanson, and A.C. Gossard, Phys. Rev. Lett. **103**, 160503 (2009).
10. G. Grynberg and C. Robbilliard, Phys. Rep. **355**, 355 (2001).
11. N. Schlosser, G. Reymond, I. Protsenko, and P. Grangier, Nature (London) **411**, 1024 (2001).
12. N.H. Dekker, C.S. Lee, V. Lorent, J.H. Thywissen, S.P. Smith, M. Drndié, R.M. Westervelt, and M.Prentiss, Phys. Rev. Lett. **84**, 1124 (2000).
13. M. Saffman, T. G. Walker and K. Mømer, Rev. Mod. Phys **82**, 2313 (2010).
14. M.D. Lukin, M. Fleischhauer, and R. Cote, Phys. Rev. Lett. **87**, 037901 (2001).
15. P.O. Schmidt, T. Rosenband, C. Langer, W.M. Itano, J.C. Bergquist, and D.J. Wineland, Science **309**, 749(2005).
16. P. Rabl and P. Zoller, Phys. Rev. A **76**, 042308 (2007).
17. M. Nielsen and I. Chuang, Quantum Computation and Quantum Information (Cambridge University, Cambridge, Englandd 2000).
18. D. Jaksch, J.I. Cirac, P. Zoller, S.L. Rolston, R. Côté, and M.D. Lukin, Phys. Rev. Lett. **85**, 2208 (2000)
19. L. Isenhower, E. Urban, X. L. Zhang, A. T. Gill, T. Henage, T. A. Johnson, T. G. Walker, and M. Saffman, Phys. Rev. Lett. **104**, 010503 (2010)
20. Marco Anderlini, P.J. Lee, B.L. Brown, J. Sebby-Strabley, W. D. Phillips, and J. V. Porto, Nature (London) **448**, 452 (2007).
21. T. F. Gallagher, *Rydberg Atoms* (Cambridge University Press, New York, 1994).
22. G. Morigi and H. Walther, Eur. Phys. J. D. **13**, 261 (2001)
23. D.F.V. James, Appl. Phys. B. **66**, 181 (1998)
24. M. Orszag, Quantum Optics:Including Noise Reduction, Trapped Ions, Quantum Trajectories, and Decoherence (Springer-Verlag Berlin Heidelberg 2000).
25. M. Saffman and T.G. Walker, Phys. Rev. A **72**, 022347 (2005).
26. G. Morigi, J. Eschner, J.I. Cirac, and P. Zoller, Phys. Rev. A **59**, 3797 (1999).
27. C. Monroe, D. M. Meekhof, B. E. King, W. M. Itano, D. J. Wineland, Phys. Rev. Lett. **75**, 4714 (1995).
28. D. J. Wineland *et al.*, J. Res. Nat. Inst. Stand. Technol. **103**, 259 (1998).
29. D. M. Meekhof, C. Monroe, W. M. Itano, B. E. King, and D. J. Wineland, Phys. Rev. Lett. **76**, 1796 (1996).
30. C. I. Cirac, P. Zoller, Phys. Rev. Lett. **74**, 4091 (1995).
31. Ralchenko, Yu., Kramida, A.E., Reader, J., and NIST ASD Team (2011). NIST Atomic Spectra Database (ver. 4.1.0), [Online]. Available: http://www.nist.gov/pml/data/asd.cfm
32.
33. M.D. Barrett *et al.*, Phys. Rev. A **68**, 042302 (2003).
    W. H. Oskay *et al.*, Phys. Rev. Lett. **97**, 020801 (2006).
34. A. Gaëtan, Y. Miroshnychenko, T. Wilk, A. Chotia, M. Viteau, D. Comparat, P. Pillet, A. Browaeys, and P. Grangier, Nat. Phys. **5**, 115 (2009).